Biogeochemistry
DOI 10.1007/s10533-017-0360-7

Soil organic carbon partitioning and $\Delta^{14}C$ variation in desert and conifer ecosystems of southern Arizona

Rebecca A. Lybrand · Katherine Heckman · Craig Rasmussen

Received: 2 September 2016 / Accepted: 29 June 2017

Abstract Soils are significant terrestrial carbon stores yet the mechanisms that stabilize organic carbon in mineral soil remain poorly constrained. Here, we identified climate and topographic controls on soil organic carbon storage along the Catalina Critical Zone Observatory that spans a significant range in mean annual temperature (>10 °C) and mean annual precipitation (>50 cm year^{-1}). Granitic soils were collected from divergent summit and convergent footslope positions in desert scrub, pine, and mixed conifer systems. Physical soil carbon distribution was quantified using a density and sonication technique to obtain the "free," "occluded," and heavy "mineral" soil carbon pools. We examined bulk soil (<2 mm) and density fractions using total carbon (%), stable isotopic composition ($\delta^{13}C$), and radiocarbon analyses ($\Delta^{14}C$). Desert scrub soils stored minimal soil carbon (<1% by weight) that was partitioned to the heavy mineral pool. Surprisingly, we identified depleted $\Delta^{14}C$ in the bulk soil (−9 to −66‰) and mineral C fractions (−72 to −90‰) from subsurface weathered granite in the desert system. The transition to the productive P. pine ecosystem was met with more soil C (>3%) that partitioned evenly between the free light and mineral fractions. Soil C in the P. pine system also reflected the impact of a moderate severity fire in 2002 that led to modern $\Delta^{14}C$ values for bulk soil and density fractions. The mixed conifer system contained a greater proportion of passive occluded C in the subsurface soils. We observed evidence for modern fire inputs into the surface soils of the mixed conifer system in combination with buried charcoal and occluded C associated with historic fire events. Convergent landscapes contained higher soil carbon stocks and depleted $\Delta^{14}C$ relative to adjacent divergent landscapes, suggesting a landscape-level mechanism that includes the transport, burial, and preservation of soil carbon downslope. These data sets provide insights into ecosystem- and hillslope-scale variations in soil carbon storage across semiarid to subhumid environments.

Keywords Climate · Critical zone · Desert soil · Forest soil · Soil organic carbon · Topography

Responsible Editor: Jonathan Sanderman.

Electronic supplementary material The online version of this article (doi:10.1007/s10533-017-0360-7) contains supplementary material, which is available to authorized users.

R. A. Lybrand · C. Rasmussen
Department of Soil, Water and Environmental Science, University of Arizona, Tucson, AZ 85721, USA

R. A. Lybrand (✉)
Department of Crop and Soil Science, Oregon State University, Corvallis, OR 97331, USA
e-mail: rebecca.lybrand@oregonstate.edu

K. Heckman
Northern Research Station, USDA Forest Service, Houghton, MI 49931, USA

Published online: 13 July 2017

Introduction

Soil organic carbon (SOC), the largest and most dynamic C pool on Earth's terrestrial surface (2344 Pg C; Jobbágy and Jackson 2000; Lal 2004), is an integral part of the global C cycle (Trumbore et al. 1996). Forests sequester natural and anthropogenic C as biomass and contribute inputs to belowground soil C sinks (Pacala et al. 2001; Ekblad et al. 2013). Temperate forests in the western U.S. serve as substantial soil C reservoirs (Homann et al. 2007). For example, conifer forests in Arizona and California account for ~45% of the regional belowground C budget despite occupying only a quarter of the area's land surface (Rasmussen 2006). Western US forests are susceptible to climate change because warmer temperatures and variable precipitation lend to the upward shift of warmer, drier ecosystems and the simultaneous narrowing of habitats suitable for high elevation forests (Crimmins et al. 2010). Mechanisms that preserve soil C in forested systems must be identified to better understand future trajectories of belowground C storage (Seager et al. 2007; IPCC 2013). The Sky Island region of the southwestern US connects large expanses of desert to forested ecosystems (Coronado Planning Partnership 2008), creating environmental gradients that comprise large precipitation and temperature differences over short distances (Whittaker and Niering 1965; Lybrand and Rasmussen 2015). Here, we study how mineral soil C stocks and stabilization mechanisms vary along a bioclimate gradient in Arizona.

Mechanisms of soil C stabilization encompass a set of processes that enhance the probability of SOC to remain in the system, with the stability of soil organic matter (SOM) defined as "a situation where either SOM molecular composition or concentration or both remain constant for extended periods of time (Berhe and Kleber 2013)." Selective preservation, spatial accessibility, and organo-mineral interactions are mechanisms that stabilize organic C and regulate residence time in mineral soils (Swanston et al. 2005; Von Lützow et al. 2008; Torn et al. 2009; Wagai et al. 2009). Free light, occluded, and mineral soil C pools preserved by these mechanisms show marked differences in organic C content, chemical composition, isotopic abundance, and residence time (Golchin et al. 1994; Sohi et al. 2001; Swanston et al. 2002; Schrumpf et al. 2013). The "free" or "light" fraction (f-LF) is the unprotected, inter-aggregate C pool that is plant-like in nature, and exhibits the shortest mean residence times in soils (Golchin et al. 1994; Torn et al. 2009). The "occluded" soil C pool (o-LF) comprises the "light" fraction material that is physically occluded and made spatially inaccessible to microbes and enzymes through aggregation or other mechanisms (Von Lützow et al. 2008). The "heavy" mineral fraction (HF) encompasses mineral-associated C that varies in age and stability (Swanston et al. 2005).

Bulk soil C stocks vary with climate (Trumbore et al. 1996; Kane et al. 2005) and land cover type (Trumbore et al. 1995; Jobbágy and Jackson 2000; Rasmussen and White 2010). Studies along environmental gradients document substantial, non-linear increases of soil C in wetter, more productive ecosystems (Landi et al. 2003; Dai and Huang 2006; Homann et al. 2007; Djukic et al. 2010; Meier and Leuschner 2010) and provide insight into how soils might respond to climate change (Dahlgren et al. 1997). The non-linear increases in soil C have been attributed to interactions among precipitation, temperature, vegetation composition, and decomposition rates along elevation transects in the Austrian Limestone Alps (Djukic et al. 2010), the Sierra Nevada, USA (Dahlgren et al. 1997; Rasmussen et al. 2007, 2010), the Solling Mountains and Thuringia Basin of Central Germany (Meier and Leuschner 2010), and in six geographical regions of China (Dai and Huang 2006). The Sky Islands of the southwestern US exhibit similar non-linear increases in soil C stocks that reflect greater moisture availability and higher rates of net primary productivity (Whittaker and Niering 1975). Soil C stocks along such gradients also vary with landscape position (Lybrand and Rasmussen 2015), indicating that variability in soil C is driven by local topography and non-linear increases with climate.

Landscape position contributes to complex catchment-scale variation in soil C storage when overlaid with regional bioclimatic controls on soil C stocks (Schimel et al. 1985; Hook and Burke 2000; Rosenbloom et al. 2006; Berhe et al. 2008; Webster et al. 2008; Torn et al. 2009; Hancock et al. 2010). Soil C concentrations can be ~2–3 times higher in convergent, depositional footslope landscapes compared to adjacent midslope and divergent summit positions as

observed in catena studies from the western US and Northern Territory, Australia (Schimel et al. 1985; Yoo et al. 2006; Berhe et al. 2008, 2012; Hancock et al. 2010). The variability of soil C with terrain is associated with the downslope movement of water, clay, organic matter, dissolved organic carbon (DOC), and nutrients (Birkeland 1999). This re-distribution of water and soil materials contributes to hillslope scale differences in vegetation composition, biomass accretion, and C inputs to the subsurface (Gessler et al. 1995; Nicolau et al. 1996). A process-response model demonstrated a high degree of variability in soil C distribution with terrain, where large (>50%) percentages of C were predicted in deep, lowland soils as a result of downslope transport and burial (Rosenbloom et al. 2006). Measured and modeled observations of soil C storage indicate that preservation mechanisms and turnover times require examination across three-dimensional space.

The nature of soil organic matter in fire-prone forests of the western US reflects intricate soil-landscape relationships (e.g., Gonzalez-Perez et al. 2004; Berhe et al. 2012; Doetterl et al. 2016). A review of SOC cycling in dynamic landscapes describes eroding hillslopes as positions that comprise young, labile pools of SOC with limited subsurface accumulation in soils where fresh SOC inputs result from net primary production (Doetterl et al. 2016). Conversely, soils in depositional positions contain large subsurface C stocks that represent old, stable pools of SOC where burial plays a dominant role in C storage processes. The amount of SOC buried in a depositional landscape coincides with environmental site conditions as well as the rate and timing of burial whereas the composition of the buried SOC can vary (Berhe et al. 2012), ranging from C-rich surface soils, to C-depleted subsurface materials, to the integration of charred materials following wildfire (Doetterl et al. 2016). A knowledge gap exists in understanding the relative partitioning of free, occluded, and mineral-associated SOC pools to erosional and depositional landscape positions, particularly in fire-impacted systems.

The Sky Island region of the southwestern US has experienced wildfire as an active, ecosystem altering process on decadal to centennial timescales (Baisan and Swetnam 1990; Farris et al. 2010). Patterns of fire frequency and extent are driven by moisture availability, topography, and vegetation characteristics of a given landscape (van Wagtendonk et al. 1998; Stephens et al. 2004; Iniguez et al. 2008, 2016). Tree-ring reconstructions for the Rincon Mountain Wilderness area in Arizona indicate that large surface fires (>200 ha) burned forested landscapes every decade over the last several hundred years (Baisan and Swetnam 1990). We predict that both modern and historic fire events contribute to the complex nature of soil C pools in the Sky Island region, particularly in the productive conifer systems where post-fire erosion and burial also regulate soil C preservation (Carroll et al. 2007). Quantifying the variation in the partitioning and storage of SOC along climate and topographic gradients requires recognition of modern and historic fire events that have and continue to impact ecosystems.

The objective of this study was to quantify how soil C stocks vary with depth, topography, and climate in the transition from desert scrub to fire-prone forests in the Catalina Critical Zone Observatory (C-CZO) of southern Arizona, USA. We sampled surface and subsurface mineral soils from two catena end members in desert scrub, pine, and mixed conifer systems to address the combined impacts of climate, vegetation, and landscape position on soil C stabilization. Previous work suggested that footslope positions concentrate twice as much soil C as adjacent summit landscapes in these environments (Lybrand and Rasmussen 2015). However, the residence time of this C is unknown, as are the dominant preservation mechanisms in each ecosystem. The impact of historic and modern fire regimes on the partitioning and storage of SOC is also poorly understood in the Sky Island region. We measured organic C and nitrogen (N), $\delta^{13}C$, and $\Delta^{14}C$ for bulk soil (<2 mm) and soil C fractions obtained through density separation. We hypothesized that climate exhibits the strongest control on physical C distribution and $\Delta^{14}C$ in the Catalina CZO. We expected soil C in the dry, hot desert soils to stabilize as organo-mineral complexes with short mean residence times, whereas fire-prone conifer systems would contain stable soil C preserved as occluded char material. We further hypothesized that landscape position would act as a local control on soil C distribution with greater quantities of stable, old carbon in water-gathering convergent areas; an observation predicted to increase proportionally with moisture availability along the environmental gradient.

Methods

Study site

The Catalina Critical Zone Observatory in Arizona encompasses an environmental gradient spanning mean annual temperatures of 21–9 °C and precipitation ranges of 250–950 mm year^{-1}. (Figure 1a). Estimates of net primary productivity range from 92 to 140 g m^{-2} year^{-1} in desert ecosystems compared to 1050–1150 g m^{-2} year^{-1} in high-elevation conifer forests (Whittaker and Niering 1975). Vegetation types include desert scrub (*Carnegiea gigantean, Fouquieria splendens, Ferocactus wislizeni, Agave schotti,* and *Agave palmeri*) at 800 m above sea level (m a.s.l.), to conifer forest dominated by *Pinus Ponderosa* at ~2250 m a.s.l., to mixed conifer forest comprised of *Pseudotsuga menziesii, Pinus ponderosa, and Abies concolor* at 2500 m a.s.l. (Table 1) (Whittaker and Niering 1965; Whittaker et al. 1968). Desert scrub, P. pine, and mixed conifer sites were selected from north-facing hillslopes on granitic parent materials of similar mineralogical composition (Lybrand and Rasmussen 2014). The Monitoring Trends in Burn Severity (MTBS) database was used to examine the modern fire history of our sites by identifying fires that were greater than 1000 acres in size and occurred from 1984 to the present (mtbs.gov; Eidenshink et al. 2007). The desert scrub site showed no recent wildfire activity whereas the P. pine site burned with moderate severity during the Bullock Fire in 2002 and the mixed conifer site experienced a low severity burn from the Aspen Fire in 2003.

Aridity class—defined as the ratio of mean annual precipitation (MAP) to potential evapotranspiration (PET)— was extracted for each ecosystem from the PRISM climate dataset (prism.oregonstate.edu; Daly et al. 2015) and sites classified as water-limited, MAP/PET <1, or energy-limited, MAP/PET >1. Potential evapotranspiration was calculated following Thornthwaite and Mather (1957). The desert scrub ecosystem had a MAP/PET of 0.5 compared to 1.3 and 1.5 in the P. pine and mixed conifer ecosystems, respectively (Table 1; Lybrand and Rasmussen 2015). The desert scrub soils have an aridic soil moisture regime and thermic soil temperature regime that transitions to an ustic soil moisture regime and mesic soil temperature regime in the P. pine and conifer sites (Soil Survey Staff 2010).

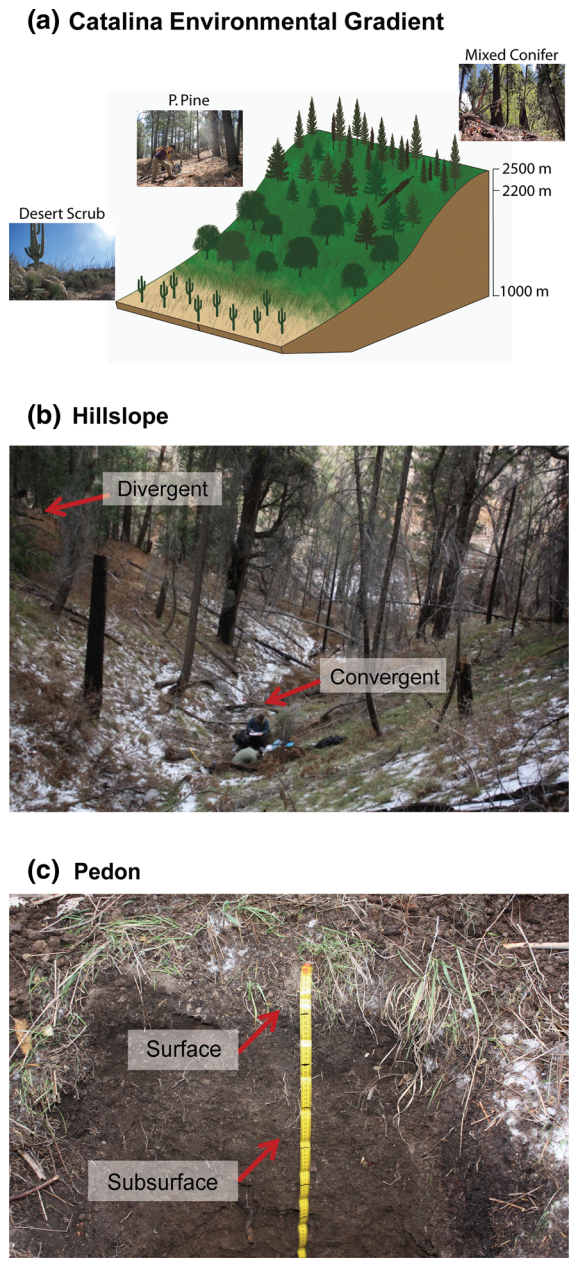

Fig. 1 **a** A schematic of the field sites along the Santa Catalina environmental gradient where soils were collected from **b** divergent-convergent landscape positions along a hillslope within each field site (example in this figure is from the mixed conifer site). **c** Surface and subsurface soils were collected for density separations and radiocarbon analyses

Sampling scheme

We sampled pedons from two divergent and two convergent landscape positions within each ecosystem, for a total of twelve pedons (Fig. 1b). Soils from

Table 1 Field site characteristics and soil pH data for the desert scrub, P. pine, and mixed conifer soil pedons in the Catalina Critical Zone Observatory. Field site characteristics include mean annual temperature (MAT), mean annual precipitation (MAP), and major overstory vegetation type. Soil pH data are reported for convergent and divergent landscape positions as depth-weighted averages ±2σ. Field site characteristics and soil pH data were published previously for the desert scrub and mixed conifer sites (Lybrand and Rasmussen 2014, 2015)

Field Site	Landscape position	Elevation (m)	MAT (°C)	MAP (cm)	MAP/PET ratio	1:1 Soil: water pH ± 2σ	1:1 Soil: 1 M KCl pH ± 2σ	Dominant vegetation type
Desert Scrub	Convergent	1092	18	45	0.53	6.2 ± 0.38	5.0 ± 0.94	Saguaro (*Carnegiea gigantean*), Ocotillo (*Fouquieria splendens*), Acacia, Arizona Barrel Cactus (*Ferocactus wislizeni*), and Agave (*Agave schotti, Agave palmeri*)
Desert Scrub	Divergent					6.2 ± 0.00	4.8 ± 0.10	
Ponderosa Pine	Convergent	2230	10	91	1.26	5.5 ± 0.18	4.0 ± 0.06	Ponderosa pine (*Pinus ponderosa*) with sparse Douglas fir (*Pseudotsuga menziesii*)
Ponderosa Pine	Divergent					5.6 ± 0.46	4.2 ± 0.06	
Mixed Conifer	Convergent	2408	9.4	95	1.47	5.6 ± 0.70	4.3 ± 0.46	Douglas fir (*Pseudotsuga menziesii*), Ponderosa Pine (*Pinus ponderosa*) and White fir (Abies concolor)
Mixed Conifer	Divergent					5.7 ± 1.1	4.4 ± 1.2	

water-shedding, divergent summits and adjacent water-gathering, convergent footslopes were sampled from transects perpendicular to the slope to minimize differences in colluvial deposition (Birkeland 1999). Soils were collected by genetic horizon to the depth of refusal, air-dried, sieved to <2 mm to obtain the fine-earth fraction, and prepared for total C and N analysis. A subset of surface (0–10 cm) and subsurface (30-40 cm) samples from one divergent-convergent pair in each ecosystem were used to examine soil C partitioning in density fractions (Fig. 1c).

Density fractions separation

Density separation and sonication were used to obtain three operationally defined pools of soil C: the f-LF, or non-mineral associated C isolated by flotation in a dense liquid; the o-LF, or soil C separated by flotation in a dense liquid after sonication that includes C either occluded within aggregates and/or coated with minerals; and HF, the remaining soil C that is associated directly with mineral surfaces and not isolated by density flotation/sonication (Fig. A1) (Golchin et al. 1994; Sohi et al. 2001; Rasmussen et al. 2005). In short, 30 g of bulk soil (<2 mm) was suspended for 24 h in sodium polytungstate adjusted to a density of 1.65 g cm^{-3}. The f-LF separated from the sample following centrifugation was collected with the supernatant. The remaining bulk soil was dispersed using ultrasonic energy at 1500 J g^{-1} soil with a Branson 450 Sonifier calibrated with DI water (North 1976). The sonication step separated the o-LF following the steps for the f-LF. The remaining heavy material was the HF. After release from the bulk soil, each fraction was rinsed with aliquots of 0.01 M $CaCl_2$ and DI water over 0.8 μm filters, and dried at 40 °C.

Additional soil C data

We compiled percent C for >50 surface soils in the Santa Catalina Mountains and nearby Rincon Mountains to provide context for our work and to expand the scope of the sample set (Fig. 2). Total organic C percentages were extracted from published data for 19 surface soil samples from the north and south sides of the SCM (Whittaker et al. 1968), 19 surface soil samples from the south side of the SCM (Galioto 1985), 12 surface soil samples from the Rincon Mountains that are adjacent and geologically similar to the SCM (Rasmussen 2008), and 3 surface soil samples from a mixed conifer forest in the SCM (Heckman et al. 2014). To expand our sample size, we integrated additional $\Delta^{14}C$ data into our interpretations (e.g., Figure 4d) including 8 bulk soil radiocarbon data points for granitic soils in the Rincon Mountains

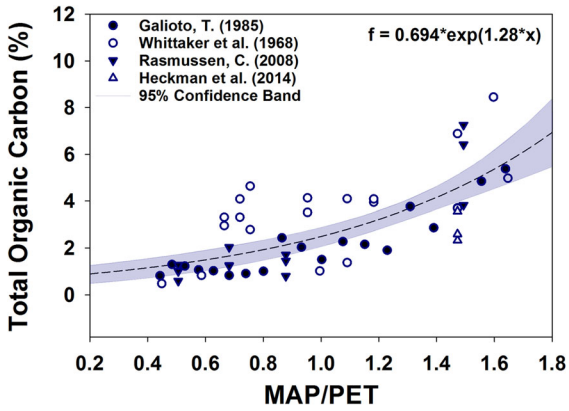

Fig. 2 Total carbon percentages for surface soils of sites spanning the Santa Catalina and Rincon environmental gradients in Arizona. The figure includes data sets adapted from Galioto (1985), Whittaker et al. (1968), Rasmussen (2008), and Heckman et al. (2014)

(Rasmussen 2008) and 3 bulk soil and density fraction data sets from Heckman et al. (2014).

Soil C and N

Percent soil organic C, percent soil organic N, and the stable isotopic composition of C ($\delta^{13}C$) and N ($\delta^{15}N$), were measured on all bulk soil (<2 mm) and density fraction samples at the University of Arizona's Environmental Isotope Laboratory. Approximately 3.5 g of sample was ground in a steel canister containing 3 tungsten carbide ball bearings that was placed on a ball-mill for 10 min. If too little sample was recovered for ball-milling (i.e., f-LF and o-LF fractions), the material was homogenized using a mortar and pestle. Elemental analyses were performed on a Finnigan Delta Plus XL (Thermo Fisher Scientific, Bremen, Germany) coupled to an elemental analyzer (Costech Analytical Technologies Inc., Valencia, CA, USA).

Percent C and percent N were reported on an oven-dry basis and assumed equivalent to organic C and N because carbonates were not detected in the samples. Soil C stocks (kg m^{-2}) for the *i*th horizon were determined according to:

$$C_i\left(\text{kg m}^{-2}\right) = \left(\frac{\rho_s \times z_i \times (1 - V_r) \times C\%}{100}\right) \times 10 \quad (1)$$

where ρ_s is the soil bulk density, z_i is horizon thickness, V_r is volumetric rock fragment, and C % is percent C. The C_i values were calculated for each horizon. The ρ_s and V_r inputs were estimated following the respective methods of Rawls (1983) and Torri et al. (1994), as outlined previously (Lybrand and Rasmussen 2015).

Soil C concentration (kg m^{-3}) was calculated as:

$$C_i\left(\text{kg m}^{-3}\right) = \left(\frac{C_i\left(\text{kg m}^{-2}\right)}{z_i}\right) \quad (2)$$

where C_i represents total horizon C (kg m^{-2}) as determined in Eq. 1 and z_i is total horizon thickness. The C_i (kg m^{-3}) values were reported on a horizon basis.

Bulk soil C refers to the % C or C_i (kg m^{-3}) measured in the fine-earth (<2 mm) fraction for each soil horizon. Partitioned C refers to the proportion of total bulk C distributed in the f-LF, o-LF, or HF that was density separated from a subset of surface (0–10 cm) or subsurface (30–40 cm) soil samples.

Radiocarbon analyses

Surface and subsurface bulk soil (<2 mm) and density fraction samples were graphitized for radiocarbon analysis at the Lawrence Livermore National Laboratory. Briefly, each ground sample (~45 mg) was combusted in a sealed glass test tube containing CuO and Ag to generate CO_2 (g) that was subsequently reduced to graphite by heating with H_2 (g) and a Fe catalyst as described by Vogel (1987). Radiocarbon measurements of the resulting graphite targets were performed by accelerator mass spectrometry at the Center for Accelerator Mass Spectrometry (CAMS), Lawrence Livermore National Lab (Davis et al. 1990). The resulting measurements were corrected for radioactive decay through normalization to the absolute activity of Oxalic Acid I— an international radiocarbon standard. Quality control was accomplished by analyzing a set of additional well-established radiocarbon standards (Oxalic Acid II, Australian National University sucrose, and TIRI wood) with the sample unknowns. Radiocarbon contents are reported as fraction modern (Fm) and in units of $\Delta^{14}C$ for each bulk soil and C fraction analyzed (Table A1). Analytical errors of the measured samples averaged ±0.0031 $Fm^{14}C$ or ±3.1‰ $\Delta^{14}C$.

Four DOC samples were also collected from lysimeters installed in convergent landscapes at the mixed conifer site. Soil water was sampled from the

soil-saprock boundary where unexpectedly modern radiocarbon values in bulk soil C and f-LF were observed. Water samples were filtered through 0.45 µm nylon filters and transported on ice to Lawrence Livermore National Laboratory where they were subsequently lyophilized, graphitized, and measured by AMS as described above.

Statistical analyses

Correlation analyses among environmental variables, soil properties, and C variables were performed in JMP V.11.0.0 (SAS Institute Inc., NC, USA) (Table A2, Table A3). Most variables required natural log transformation to achieve a normal distribution. The bulk soil correlation matrix integrated pH 1:1 KCl, C:N ratio, C (kg m^{-2}), and $\delta^{13}C$ (‰) data from 49 soil horizons sampled in our study across the SCM desert (n = 13), pine (n = 16), and mixed conifer sites (n = 20). Clay (%), sand (%), C (%), depth, and MAP/PET were analyzed using 60 samples from 49 soil horizons in our SCM study, 3 SCM mixed conifer soil horizons (Heckman et al. 2014), and 8 Rincon Mountain soil horizons (Rasmussen 2008). The bulk soil $\Delta^{14}C$ variable contained data from 35 samples including 24 SCM soil horizons in our study, 3 SCM mixed conifer soil horizons (Heckman et al. 2014), and 8 Rincon soil horizons (Rasmussen 2008).

The sampling design with only two soil profiles per landscape position per ecosystem does not allow use of a full factorial ANOVA for testing differences among all main effects of ecosystem and landscape position. To address this limitation, the data were pooled across the main effects of ecosystem (n = 3) and landscape position (n = 2). We tested for differences in % C, C:N, and isotopic composition using one-way ANOVA.

Results

Soil C and N variation with climate and landscape position

Surface soil % C increased exponentially with moisture availability along the Santa Catalina and Rincon environmental gradients ($r^2 = 0.53$, $P < 0.0001$) from <1% in the desert sites to >8% in mixed conifer forest (Fig. 2). Climate, represented here as MAP/PET, exhibited the strongest positive correlations with soil C stocks, soil C:N, silt, and clay (Table A2, A3; Whittaker et al. 1968); relationships most pronounced in the convergent water-gathering landscape positions (Lybrand and Rasmussen 2015). The ratio of convergent to divergent SOC stocks also increased with MAP/PET, indicating a greater proportion of SOC stored in convergent landscapes for conifer versus the desert scrub sites (Fig. 3).

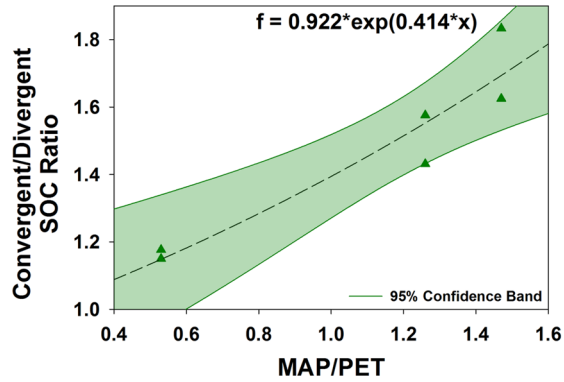

Fig. 3 A convergent to divergent ratio of soil organic carbon volumetric concentrations (kg m^{-3}) as a function of MAP/PET. The data points represent pedon averages that are referenced from Table 2 herein and Fig. 4 in Lybrand and Rasmussen (2015)

Soil C partitioning, isotopic composition, and concentration in density fractions

The density fraction data pooled across all sites indicated significant variation among fractions regardless of ecosystem type with respect to partitioned C ($P < 0.0001$), $\delta^{13}C$ ($P = 0.0390$), C:N ($P < 0.0001$), and $\Delta^{14}C$ ($P = 0.0298$) (Fig. 4a–d). The greatest proportion of total C was distributed to the mineral fraction with an average of 56 ± 20%, compared to 36 ± 17% in the f-LF, and 9 ± 8% in the o-LF fractions (Fig. 4a). The HF was generally enriched in $\delta^{13}C$ relative to the o-LF and f-LF fractions (Fig. 4b) and C:N was highest in the o-LF fractions (Fig. 4c). The density fractions showed large ranges in $\Delta^{14}C$ content with distributions from −10‰ to 115‰ in the f-LF, −91‰ to 116‰ in the o-LF, and −90‰ to 110‰ in the HF. The f-LF was most enriched in $\Delta^{14}C$, averaging 73 ± 33‰ which contrasted respective mean values of 27 ± 64‰ and 29 ± 55‰ for the o-LF and HF (Fig. 4d).

Table 2 Average soil C properties ± standard deviation (SD) for free light, occluded light, and heavy mineral density fractions as pooled by ecosystem. Density fractions from desert scrub, P. pine, and mixed conifer ecosystems were tested using One−way ANOVA with n = 4 pedons analyzed within each grouping. Means followed by the same letter within a field property for a given density fraction are not significantly different (Tukey's test, $p < 0.05$)

Property	Free light fraction (f-LF)				Occluded light fraction (o-LF)				**Heavy Mineral Fraction (HF)**			
	Desert mean ± SD	P. Pine mean ± SD	Mixed conifer mean ± SD	*P* value	Desert mean ± SD	P. Pine mean ± SD	Mixed conifer mean ± SD	P-value	Desert mean ± SD	P. Pine mean ± SD	Mixed Conifer mean ± SD	P-value
Partitioned Carbon (% by mass)	20 ± 9.1^{A}	51 ± 10.2^{B}	$37 \pm 17^{A,B}$	0.0205	3 ± 3.6^{A}	7.5 ± 4.20^{A}	15 ± 9.8^{A}	0.0702	78 ± 12^{A}	42 ± 10.7^{B}	48 ± 14^{B}	0.0059
$\delta^{13}C$ (‰)	-25.2 ± 0.13^{A}	-22.8 ± 0.61^{B}	-24.8 ± 0.69^{A}	0.0003	-22.8 ± 0.21^{A}	-24.6 ± 0.38^{B}	-24.7 ± 0.48^{B}	.0019	-21.3 ± 1.24^{A}	-23.7 ± 0.78^{B}	-24.2 ± 0.66^{B}	0.0042
$\Delta^{14}C$ (‰)	82.6 ± 22.9^{A}	86.1 ± 7.70^{A}	53.8 ± 54.9^{A}	0.3895	101 ± 20.4^{A}	53.7 ± 39.2^{A}	-2.53 ± 76.9^{A}	0.1635	-16.8 ± 76.0^{A}	50.8 ± 47.3^{A}	32.0 ± 38.0^{A}	0.2650
Total Carbon (%)	24.2 ± 1.84^{A}	32.3 ± 3.31^{B}	35.8 ± 1.39^{B}	0.0002	8.80 ± 2.55^{A}	39.4 ± 1.48^{B}	42.0 ± 1.72^{B}	<0.0001	0.32 ± 0.11^{A}	0.53 ± 0.35^{A}	1.46 ± 1.03^{A}	0.0664
C:N Ratio (mass ratio)	17.3 ± 1.56^{A}	34.3 ± 6.47^{B}	36.1 ± 4.49^{B}	0.0005	11.8 ± 1.27^{A}	38.4 ± 3.18^{B}	41.2 ± 9.71^{B}	0.0035	8.30 ± 0.92^{A}	$11.5 \pm 3.18^{A,B}$	17.0 ± 3.89^{B}	0.0074

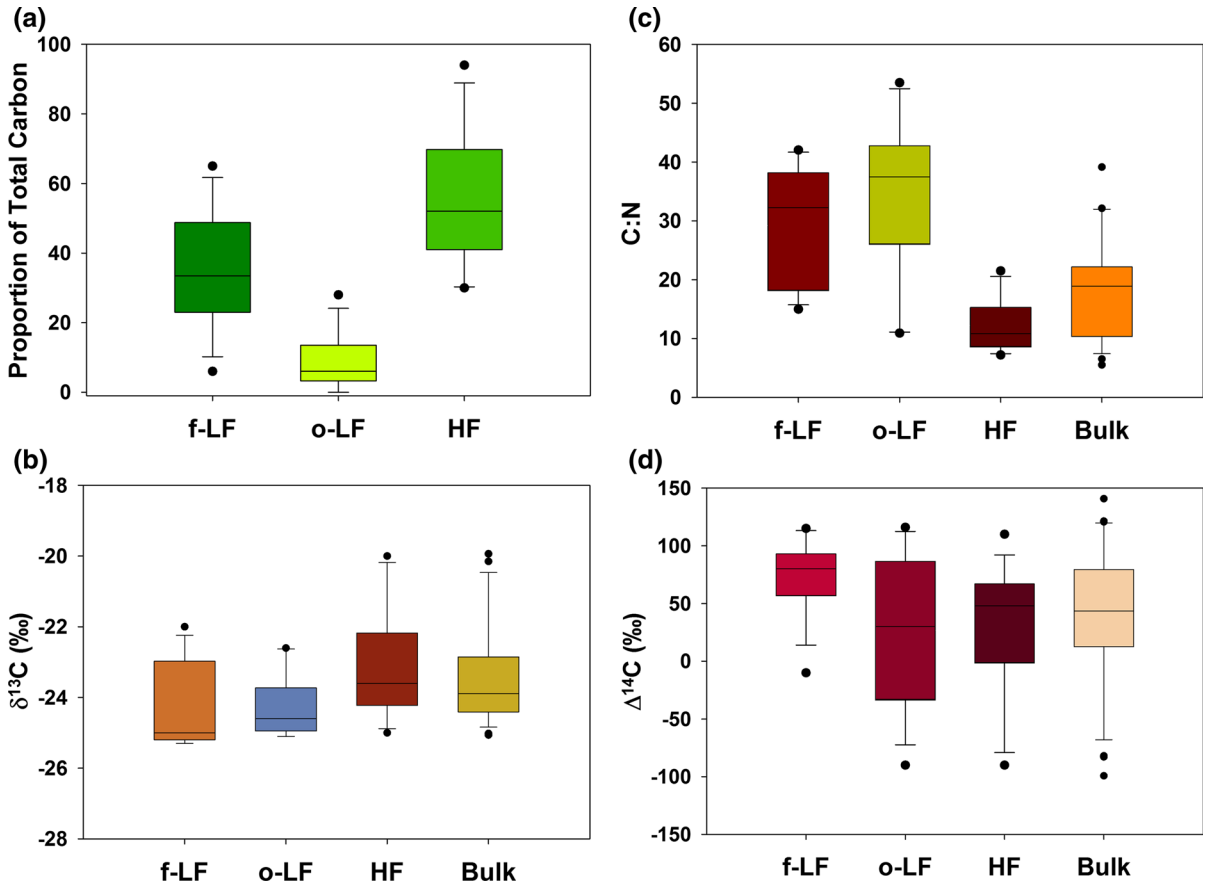

Fig. 4 Soil carbon properties across the free light (f-LF), occluded light fraction (o-LF), and heavy mineral fractions (HF) for the Santa Catalina Mountain sites. Soil carbon data sets include the following: **a** partitioned C, **b** δ13C (‰), **c** C:N, and **d** $\Delta^{14}C$ (‰). Each box plot presents the median as a *black horizontal line*. The 25th and 75th ‰ are represented as vertical boxes. The 10th and 90th ‰ are indicated by error bars

Proportion of C distributed in density fractions by ecosystem and landscape position

Relative partitioning of soil C by density fraction varied from greater than 70% to the HF of desert scrub soils to a more even distribution of SOC to the f-LF and HF in the two conifer systems (Fig. 5a–c). Visual differences in the density fractions were also noted among ecosystems (Fig. A1). The desert soils contained finer plant materials in the f-LF and lighter colored organics in the o-LF; the conifer soils had coarser plant parts in the f-LF and black, fine-grained organics in the o-LF. The mixed conifer soils contained a greater proportion of C in the o-LF relative to lower elevation sites, particularly in the convergent positions.

The desert, P. pine, and mixed conifer soils presented contrasting hillslope scale trends in soil C distribution (Fig. 5a–d). The desert scrub soils contained the highest proportion of soil C in the HF at both landscape positions (Fig. 5a). Soil C in the desert sites showed a greater partitioning to the f-LF in divergent sites versus adjacent convergent sites and a similar distribution to the o-LF between the two positions. Soil C in the P. pine soils was distributed evenly between the f-LF and HF in the divergent soils compared to convergent positions where a greater percentage of soil C partitioned to the f-LF (Fig. 5b). The partitioning of soil C to the o-LF fractions was the same between landscape positions in the P. pine sites. Occluded soil C in convergent sites was two times greater than divergent sites in the mixed conifer soils.

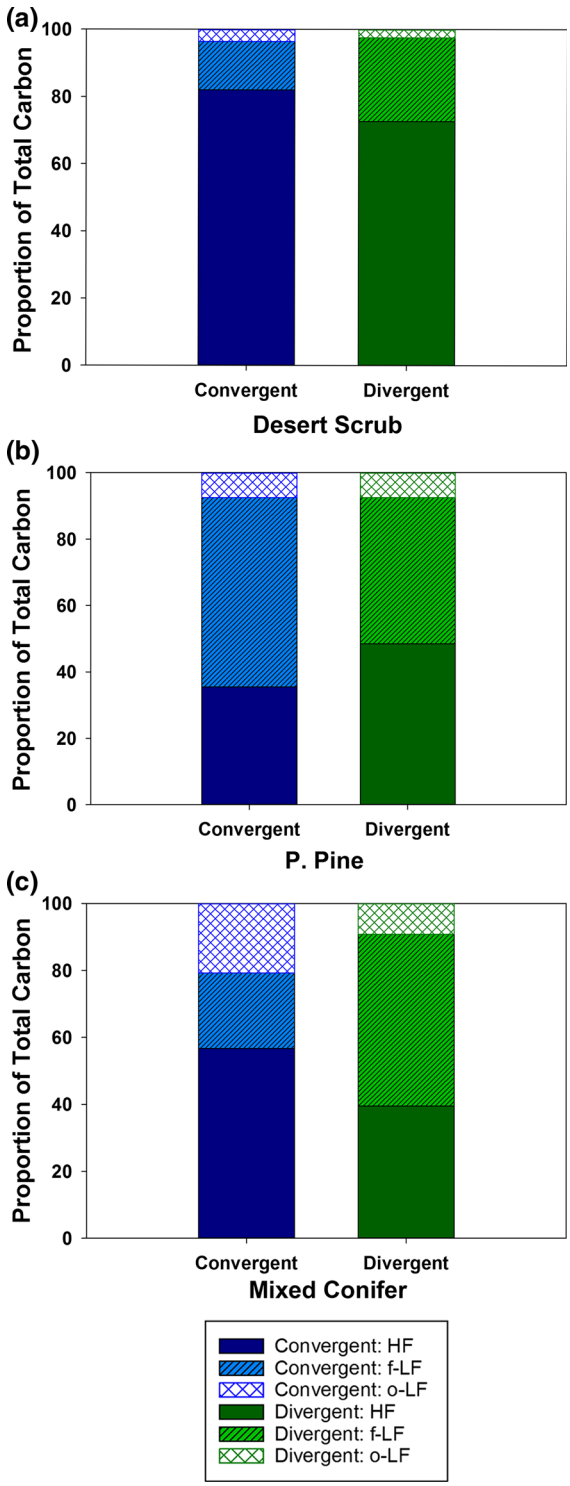

Fig. 5 Partitioning of soil organic carbon into free light (f-LF), occluded light fraction (o-LF), and heavy mineral fractions (HF) extracted from bulk soils in the **a** desert scrub, **b** P. pine, and **c** mixed conifer field sites

Furthermore, divergent soils from the mixed conifer system contained twice as much soil C in the f-LF relative to convergent positions where the greatest percentage of soil C partitioned to the HF (Fig. 5c; Table A4).

Soil C in density fractions pooled by ecosystem

Significant differences in $\delta^{13}C$ (‰), % C, and C:N were identified between the desert and conifer sites when density fractions were grouped and compared among ecosystems (Table 2). The $\delta^{13}C$ isotope composition in the f-LF, o-LF, and HF significantly varied by ecosystem and was most enriched in the o-LF and HF of the desert scrub ecosystem (Table 2). Total % C exhibited significant variation among ecosystems in the f-LF and o-LF compared to no significant differences for the HF. Similarly, C:N ratios were highest in the f-LF and o-LF fractions of the P. pine and mixed conifer soils whereas significantly lower values were observed in corresponding fractions from the desert scrub soils.

Soil radiocarbon content in desert and conifer landscapes

The desert soils presented the most depleted bulk soil $\Delta^{14}C$ of our study in both the divergent and convergent subsurface soils ($\sim$30–40 cm), with respective $\Delta^{14}C$ values of -9 ± 2.8‰ and -66 ± 2.7‰ (Table 3). The heavy mineral fractions from the subsurface desert soils also represent two of the most depleted $\Delta^{14}C$ values along the SCM gradient including -72 ± 2.6‰ and -90 ± 3.6‰ for divergent and convergent sites, respectively (Table 3; Table A1). Modern $\Delta^{14}C$ values for the f-LF and o-LF from surface soils in both landscapes were nearly identical and the subsurface soils did not contain o-LF fractions in either position. Both landscapes showed pronounced relative depletions of $\Delta^{14}C$ with depth in the HF—with decreases of 99‰ from 5 to 35 cm.

The P. pine bulk soil and density fractions had modern radiocarbon values that were all greater than 0‰, apart from one HF sample with a $\Delta^{14}C$ value of -6‰ in the subsurface soil. The $\Delta^{14}C$ values in the P. pine ecosystem varied by depth and landscape position (Table 3). Soil C in the o-LF and f-LF from the divergent soils were more enriched in $\Delta^{14}C$ with depth, where values increased by $\sim$20 and 15‰,

respectively; whereas the HF was characterized by a relative depletion in $\Delta^{14}C$ that spanned 48‰ at 0–10 cm to −6‰ at 30–40 cm. In contrast, $\Delta^{14}C$ values decreased with depth for all density fractions in the convergent position (Table 3).

The $\Delta^{14}C$ values for the mixed conifer bulk soil and density fractions were depleted at depth (Table 3), except for the convergent profile. Here, $\Delta^{14}C$ increased from −15‰ at 30–40 cm to −8.2‰ at ~120 cm which occurred at the soil-saprock boundary (based on duplicate measures from the horizon with values of 0.0 and −16.3‰; Fig. 6). The unexpected increase in radiocarbon content at the soil-saprock boundary in the convergent soil led us to examine depth profiles of $\Delta^{14}C$ at the mixed conifer site, in addition to multiple measures of DOC at subsurface depths (Table 3; Table A1). Dissolved organic C samples collected from lysimeters in convergent positions during March 2013 exhibited positive $\Delta^{14}C$ values of 43.1‰ at 39 cm and 18.5‰ at 65 cm (Fig. 6; Table A1). A third DOC sample from a 65 cm depth lysimeter in January 2013 was depleted with a $\Delta^{14}C$ value of −19.8‰.

Discussion

Soil C properties and partitioning in density fractions from desert and conifer systems

Soil C partitioning and isotopic compositions exhibited significant variation among density fractions that was most pronounced in the transition from moisture-limited desert scrub to energy-limited conifer systems (Fig. 5; Table 3). Density fractions from the desert scrub soils contained the lowest C:N of all sites, the least enriched $\delta^{13}C$ of the free light fractions, and substantial depletion in $\Delta^{14}C$ of the mineral fractions with depth (Table 2; Table A1).The majority of soil C in the desert scrub soils partitioned to the heavy mineral fractions that also presented the lowest soil C:N ratios and most depleted $\Delta^{14}C$ of the heavy fractions in the study (Table 2). Our results demonstrate that the oldest, most microbially processed soil C in the desert scrub system is preserved in the heavy mineral fraction of subsurface soils.

The conifer soils show a greater proportion of soil C distributed to the free light and occluded fractions

Table 3 Radiocarbon values ($\Delta^{14}C$) for soil organic carbon density and aggregate fractions separated from soils collected along the Santa Catalina Mountain environmental gradient in Arizona

		$\Delta^{14}C$ (‰)			
Ecosystem	Landscape position/depth	Free light	Occluded light	Heavy mineral	Bulk
Desert scrub					
	Divergent/0–10 cm	86 ± 3.1	87 ± 3.2	27 ± 3.0	51 ± 3.0
	Divergent/30–40 cm	57 ± 4.0	–	−72 ± 2.6	−9 ± 2.8
	Convergent/0–10 cm	112 ± 3.2	116 ± 3.7	67 ± 3.1	107 ± 3.2
	Convergent/30–40 cm	76 ± 3.1	–	−90 ± 3.6	−66 ± 2.7
Ponderosa pine					
	Divergent/0–10 cm	75 ± 3.1	35 ± 3.0	48 ± 3.0	78 ± 3
	Divergent/30–40 cm	89 ± 3.3	56 ± 3.1	−6 ± 2.9	66 ± 3.9
	Convergent/0–10 cm	93 ± 3.2	107 ± 3.3	110 ± 3.2	112 ± 3.3
	Convergent/30–40 cm	87 ± 3.1	16 ± 2.9	52 ± 3.0	86 ± 3.3
Mixed conifer					
	Divergent/0–10 cm	115 ± 3.3	86 ± 3.1	78 ± 3.1	96 ± 3.7
	Divergent/30–40 cm	80 ± 3.9	−90 ± 2.8	−1 ± 3.0	17 ± 3.0
	Convergent/0–10 cm	30 ± 3.1	30 ± 3.1	48 ± 3.2	41 ± 3.1
	Convergent/30–40 cm	−10 ± 3.0	−36 ± 2.9	3 ± 3.0	−15 ± 3.0
	Convergent/110–130 cm	44 ± 4.3	−35 ± 3.5	−55 ± 3.3	−8.15 ± 3.2

(Fig. 5b, c), where both present nearly identical soil C:N and $\delta^{13}C$ values, yet the occluded fractions are notably less enriched in $\Delta^{14}C$ than the free light fractions. The mineral fractions in both the P. pine and mixed conifer sites exhibited lower C:N ratios than the light fractions that suggested a greater degree of microbial processing. Low C:N ratios and enriched $\delta^{13}C$ values are indicators of decomposition in forest soils (Natelhoffer and Fry 1988; Golchin et al. 1994) where mineral fractions from grassland and conifer systems have undergone a higher degree of microbial degradation than the lighter fractions (Baisden and Parfitt 2007; Natelhoffer and Fry 1988). The lower C:N ratios in the heavy mineral fractions relative to the light fractions supported the trend of greater decomposition in heavy fractions; however, little to no difference in $\delta^{13}C$ composition was detected among the density fractions of the forest soils in this work (Table 2) or in another study of soil C from a P. pine forest in southern Arizona that reported similar $\delta^{13}C$ ranges in density fractions (Heckman et al. 2014).

Despite similarities in $\delta^{13}C$ isotopic composition, the $\Delta^{14}C$ values of the density fractions reflect substantial differences in estimated mean residence times (Table A6), likely due to the increased partitioning of charcoal inputs to occluded fractions as a result of wildfire in western US forests (Heckman et al. 2014). We observed a greater proportion of charcoal in the occluded fractions from the conifer sites compared to low elevation desert soils (Fig. A1). Our findings suggest that the physical occlusion of soil C in aggregates preserves SOC from degradation in forest soils (Wagai et al. 2009), and indicates that wildfire may play a role in the partitioning of soil C to occluded fractions in fire prone conifer systems (Heckman et al. 2014).

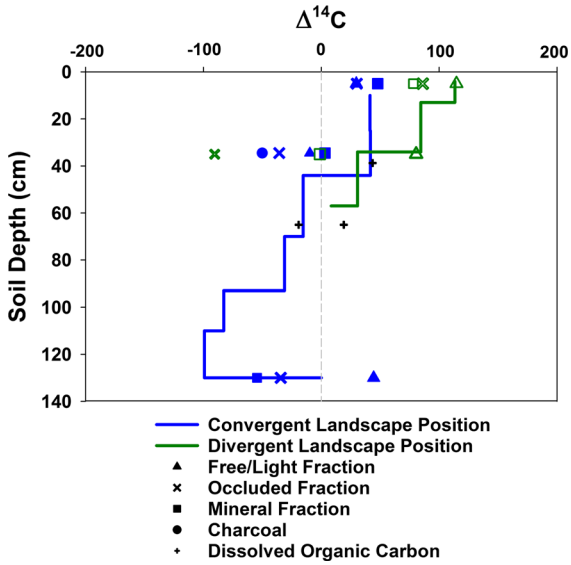

Fig. 6 Radiocarbon values of bulk soils and free light (f-LF), occluded (o-LF), and heavy mineral fractions (HF) from mixed conifer soils in the Santa Catalina Mountains, AZ

Preservation of soil C: desert scrub

Our study is one of the first to examine the variation of soil C partitioning in desert landscapes and to report depleted $\Delta^{14}C$ in the weathered granitic bedrock of a hot, water-limited desert ecosystem. We found mineral-associated C to be the largest and most stable soil C pool in the desert scrub sites with estimated mean residence times on the order of hundreds of years in the subsurface (Table A6) compared to prior work in the Sonoran Desert that documented mean residence times of 20–40 years for soil C in bulk soil and clay fractions (McClaran et al. 2008). We hypothesize that the depleted $\Delta^{14}C$ observed from the weathered bedrock in our study results from the low primary productivity of the desert scrub ecosystem. Here, limited productivity reduces the potential for soil C exchange with depth, particularly the replacement of old soil C with modern C inputs in the fractures of weathered bedrock.

Few studies have examined soil C partitioning in desert systems; however, an investigation of shrub expansion on soil C distribution found that ~88% of bulk soil C in a composite grassland profile partitioned to the heavy mineral fraction (Connin et al. 1997), which is similar to the mean of ~70% in the heavy fraction from our study. In contrast, carbon from the upper 5 cm of alluvial soil in an arid, hyperthermic Sonoran Desert system largely partitioned to the free light fraction, with little to no organic C in occluded or mineral fractions (Rasmussen and White 2010; White et al. 2009). Contrasting sampling depths may account for the difference between the prevalence of free light soil C in prior studies compared to mineral-associated soil C in our study. The soils in our systems also formed on granitic bedrock that may facilitate the differential storage of soil C in the fractures of weathered rock in contrast to soils that developed on alluvial fan surfaces.

Preservation of soil C: P. pine

Soil C partitioning in the P. pine system shifted towards a greater proportion of free light and occluded C (Table 2), with the oldest C in the occluded and mineral fractions (Table 3). The shift in soil C partitioning in our study corresponds with the transition to energy-limited ecosystems that exhibit greater above- and below-ground primary productivity (Fig. 1; Whittaker and Niering 1975). Here, larger proportions of free light and occluded C likely originate from litter and treefall C inputs in the pine ecosystem. Greater C concentrations in the mineral fraction might result from both greater C inputs to the conifer systems (Fig. 1) and the finer-textured soils in the P. pine site that facilitate a greater degree of organo-mineral interactions compared to coarser-grained desert soils (Lybrand and Rasmussen 2015). Interestingly, modern $\Delta^{14}C$ values unexpectedly dominated all of the soil C fractions from the P. pine site (Table 3; Table A1). The young mineral C indicates an active exchange of mineral-associated C with new inputs, suggesting a dynamic pool of C pool.

We hypothesize that the soil $\Delta^{14}C$ is dominated by modern C inputs from the Bullock fire in 2002 (mtbs.gov; Eidenshink et al. 2007). We assume that the moderate severity burn generated charcoal inputs comprised of modern C that originated from forest floor and understory vegetation instead of downed woody debris that would be complicated by the inbuilt age of the charcoal in a high severity, stand-replacing fire (Gavin 2001). Modern, post-fire C likely entered the P. pine system as a large influx of particulate, soluble, and charred C, as confirmed visually by the presence of a charcoal-rich organic surface horizon and char staining throughout the soil profile (Fig. A2a). The occluded fraction also appeared to be largely dominated by charred organic matter based on visual observations that are consistent with results from other Arizona conifer systems where occluded fractions were enriched in charred materials relative to bulk soils (Fig A1; Heckman et al. 2014). The relative proportion of total C partitioned to the occluded fraction was greater in the P. pine site relative to the desert scrub soils. However, the occluded C in the P. pine site did not contain the oldest C in the system as predicted, likely due to the pulse of modern C from the fire into an otherwise stable SOC pool.

Preservation of soil C: mixed conifer

Soil C in the mixed conifer system was largely partitioned to the free light and mineral fractions (Fig. 5c). Soil C in the density fractions of the mixed conifer landscapes exhibited modern $\Delta^{14}C$ values in the surface soils that we attribute to inputs from the low intensity burn during the Aspen Fire in 2003. However, we also observed a substantial shift towards greater occluded and mineral C in the mixed conifer convergent landscapes that suggests a local hillslope scale control on soil C partitioning (Fig. A2b). On average, the mixed conifer soil C exhibited the most depleted $\Delta^{14}C$ in the subsurface occluded fractions (Fig. 6; Table 3). We hypothesize that the occluded subsurface C reflects inputs from earlier wildfire events that were preserved through post-fire burial processes (Fig. A2b) as confirmed with the radiocarbon analysis of a charcoal fragment sampled at 30–40 cm depth (Fig. 6). This contrasts with the P. pine landscapes where we only saw evidence for modern inputs from a recent fire. We also did not observe a thick charcoal-rich horizon in the mixed conifer site as we did for the P. pine system (Fig. A2a, b). We speculate that the absence of the charcoal layer may arise from: a lower intensity burn at the mixed conifer site (mtbs.gov; Eidenshink et al. 2007); differences in fuel loads where long needles of P. pine forests burn quicker than shorter needles in mixed conifer forests (Iniguez et al. 2008); or that rapid post-fire erosion in the mixed conifer forest redistributed the charred layer into materials deposited in downslope positions.

The occluded fractions from the mixed conifer subsurface soils had the longest mean residence times in both landscape positions (Fig. 6). Occluded soil C represents a stable soil C pool in other forested ecosystems where turnover times range from tens to hundreds of years (Rasmussen et al. 2005; Swanston et al. 2005; Wagai et al. 2009; McFarlane et al. 2013). The fine-grained black material observed in the occluded fraction appears to be largely char (Fig. A1). Occluded C in other AZ conifer systems exhibited longer mean residence times than free light and mineral fractions, comprising 0.5–5 times more charcoal relative to bulk soil as determined by ^{13}C NMR analyses (Heckman et al. 2014).

The physical distribution and radiocarbon values of soil C in the mixed conifer system suggest a landscape level mechanism that includes the downslope

transport and burial of soil organic C (Figs. 6, A2b; Table 3). The mixed conifer convergent soils contained twice the amount of occluded C in the subsurface versus divergent soils (Table A4), suggesting greater distribution and/or preservation of occluded materials in the convergent landscapes. We predict that charred organics partitioned to the occluded fraction in this environment following wildfire activity and that the occluded materials became buried and preserved in the subsurface via bioturbation or post-fire hillslope erosional processes (Sanborn et al. 2006).

The preservation of soil C at the hillslope scale

A greater magnitude of SOC accumulated in convergent landscape positions at higher MAP/PET (Fig. 3). We attribute this to greater in situ net primary productivity in conifer systems, greater post-fire erosion rates in conifer forests compared to desert scrub sites, and greater sediment transport rates in high elevation conifer systems from bioturbation that results in proportionally more SOC storage in downslope positions. The thick convergent zone soils in the mixed conifer system corresponds to higher rates of colluvial transport and sediment deposition in the high elevation systems of the Santa Catalina and Pinaleño ranges modeled in Pelletier et al. (2013). We postulate that the SOC preserved in these transported sediments contribute to the higher convergent/divergent SOC ratios detected in the P. pine and mixed conifer soils (Fig. 3).

Density fractions from the desert scrub and mixed conifer sites show a greater partitioning of SOC to the f-LF in divergent sites compared to the HF for convergent positions (Fig. 5; Table A2). The $\Delta^{14}C$ data from the desert scrub and mixed conifer sites also reflect modern inputs to surface divergent soils and the preservation of older C in subsurface soils of depositional landscapes (Fig. 6; Table 3). We predict that the prevalence of passive C in subsurface convergent soils from the desert system results from burial by physical erosion processes related to a greater degree of bare ground exposure compared to high elevation forests. Percent vegetation cover averaged $\sim$30% in the desert scrub site compared to >85% in the conifer systems (Fig. A3; unpublished data), suggesting that the exposed desert landscapes would be susceptible to downslope erosion during high-intensity rain events. The P. Pine site reflects a more equal distribution between f-LF and HF by landscape position with a slightly greater proportion of SOC to f-LF in convergent soils compared to divergent sites. We hypothesize that younger soil C in the mixed conifer system dominates the inputs to the f-LF in divergent soils whereas convergent landscapes reflect an accumulation of older, occluded or mineral-associated SOC that is often preserved and buried following post-fire transport from upslope positions (Figs. 5, 6).

The role of dissolved organic carbon in the mixed conifer system

The bulk soil modern $\Delta^{14}C$ signal at the soil-saprock interface of the mixed conifer convergent site could be explained by the downward transport of modern dissolved organic C (Fig. 6). Modern DOC signals of soil water collected from convergent subsurface soils in the mixed conifer watershed support this hypothesis (Fig. 6; Table A1). The leaching of DOC from organic surface horizons into the mineral soil provides an important source of organic C in soils (Schiff et al. 1990; Michalzik et al. 2003; Rumpel and Kögel-Knabner 2011), where DOC retained in mineral horizons account for $\sim$22–25% of soil C stocks in temperate forests (Neff and Asner 2001; Kalbitz et al. 2005). This DOC may persist in the subsurface on decadal time scales (Sanderman and Amundson 2008). We speculate that the modern radiocarbon value at >1 m depth in the mixed conifer site results from the rapid transport of DOC through the coarse, granitic soils (<10% clay) that subsequently accumulates at the soil-saprock interface (Fig. 6).

Summary

Our results contribute to a limited body of research on soil C partitioning in desert scrub ecosystems where we identified mineral-associated C in subsurface soils that exhibited some of the most depleted $\Delta^{14}C$ in our study (−90‰). Greater primary productivity in the conifer ecosystems led to a more even partitioning of soil C between free light and heavy mineral fractions in the forest soil systems, with the greatest proportion of occluded C in mixed conifer soils. The P. pine system reflected the impact of a low-moderate severity burn from the Bullock fire in 2002 that resulted in modern $\Delta^{14}C$ values for almost all bulk C and density fraction

samples. Surface soils in the mixed conifer system also reflected inputs from a low severity burn associated with the Aspen fire in 2003; however, we also saw evidence for historic wildfire in the form of buried charcoal and occluded materials from subsurface convergent soils that were both depleted in $\Delta^{14}C$. Dissolved organic carbon was an important component of the mixed conifer system with radiocarbon data suggesting deep vertical transport and accumulation at the soil-saprock interface in convergent positions. Landscape position represented a hillslope scale control on soil C partitioning and $\Delta^{14}C$ variation in the desert scrub and mixed conifer systems, including a greater proportion of fast-cycling soil C distributed to free light fractions in divergent positions compared to more passive mineral-associated C in convergent landscapes. We attribute the landscape level controls on soil C distribution to physical erosion resulting from limited vegetation cover in desert systems and a greater degree of post-fire erosion and burial following historic and modern wildfire events in the mixed conifer system. Our results confirm the interactive role of climate, vegetation, and landscape position in preserving soil C along the Catalina environmental gradient–from mineral-associated C in the shallow soils and saprock of the desert system to a mixture of soil C partitioned to free, occluded, and mineral fractions in the productive, fire-prone conifer forests.

Acknowledgements This research was funded by NSF EAR-1123454, NSF EAR/IF-0929850, the national Critical Zone Observatory program via NSF EAR-0724958 and NSF EAR-0632516, and Geological Society of America's Graduate Student Research Grant. Logistical support and/or data were provided by the NSF supported Niwot Ridge Long-Term Ecological Research project and the University of Colorado Mountain Research Station. Radiocarbon analyses were supported by the Radiocarbon Collaborative, which is a joint program of the USDA Forest Service, Lawrence Livermore National Laboratory, and Michigan Technological University. The authors also thank Dr. S. Mercer Meding, Katarena Matos, Molly van Dop, Justine Mayo, Stephanie Castro, Christopher Clingensmith, Mary Kay Amistadi, Nate Abramson, Dr. Julia Perdrial, Stephan Hlohowskyj, and Andrew Martinez for laboratory and field assistance.

References

Baisan CH, Swetnam TW (1990) Fire history on a desert mountain range; Rincon Mountain Wilderness, Arizona, USA. Can J For Res 20:1559–1569

Baisden WT, Parfitt RL (2007) Bomb ^{14}C enrichment indicates decadal C pool in deep soil? Biogeochemistry 85:59–68

Baisden WT, Amundson R, Cook AC, Brenner DL (2002) Turnover and storage of C and N in five density fractions from California annual grassland surface soils. Glob Biogeochem Cycle 16:1117. doi:10.1029/2001GB001822

Berhe AA, Kleber M (2013) Erosion, deposition, and the persistence of soil organic matter: mechanistic considerations and problems with terminology. Earth Surf Process Landf 38:908–912. doi:10.1002/esp.3408

Berhe AA, Harden JW, Torn MS, Harte J (2008) Linking soil organic matter dynamics and erosion-induced terrestrial carbon sequestration at different landform positions. J Geophys Res 113:G04039

Berhe AA, Harden JW, Torn MS, Kleber M, Burton SD, Harte J (2012) Persistence of soil organic matter in eroding versus depositional landform positions. J Geophys Res 117:G02019

Birkeland PW (1999) Soils and geomorphology. Oxford University Press, Oxford, p 448

Carroll EM, Miller WW, Johnson DW, Saito L, Qualls RG, Walker RF (2007) Spatial analysis of a large magnitude erosion event following a Sierran wildfire. J Environ Qual 36:1105

Connin SL, Virginia RA, Chamberlain CP (1997) Carbon isotopes reveal soil organic matter dynamics following arid land shrub expansion. Oecologia 110:374–386

Coronado Planning Partnership (2008) State of the Coronado National Forest: an assessment and recommendations for the 21st Century. www.skyislandaction.org

Crimmins TM, Crimmins MC, Bertelsen CD (2010) Complex responses to climate drivers in onset of spring flowering across a semi-arid elevation gradient. J Ecol 98:1042–1051. doi:10.1111/j.1365-2745.2010.01696.x

Dahlgren RA, Boettinger JL, Huntington GL, Amundson RG (1997) Soil development along an elevational transect in the western Sierra Nevada, California. Geoderma 78:207–236

Dai W, Huang Y (2006) Relation of soil organic matter concentration to climate and altitude in zonal soils of China. Catena 65:87–94

Daly C, Smith JI, Olson KV (2015) Mapping atmospheric moisture climatologies across the conterminous United States. PLoS ONE 10(10):e0141140

Davis JC, Proctor ID, Southon JR, Caffee MW, Heikkinen DW, Roberts ML, Moore TL, Turteltaub KW, Nelson DE, Loyd DH, Vogel JS (1990) LLNL/UC AMS facility and research program: Proc. 5th International Conference on Accelerator Mass Spectrometry, Paris. Nucl Instruments Methods Phys Res 269–272

Djukic I, Zehetner F, Tatzber M, Gerzabek MH (2010) Soil organic-matter stocks and characteristics along an Alpine elevation gradient. J Plant Nutr Soil Sci 173:30–38

Doetterl S, Berhe AA, Nadeu E, Wang Z, Sommer M, Fiener P (2016) Erosion, deposition and soil carbon: a review of process-level controls, experimental tools and models to address C cycling in dynamic landscapes. Earth Sci Rev 154:102–122

Eidenshink J, Schwind B, Brewer K, Zhu Z-L, Quayle B, Howard S (2007) A project for monitoring trends in burn severity. Fire Ecol Spec Issue 3:3–21

Ekblad et al (2013) The production and turnover of extramatrical mycelium of ectomycorrhizal fungi in forest soils: role in carbon cycling. Plant Soil 366:1–27. doi:10.1007/s11104-013-1630-3

Farris CA, Baisan CH, Falk D, Yool SR, Swetnam TW (2010) Spatial and temporal corrobation of a fire-scar based fire history in a frequently burned ponderosa pine forest. Ecol Appl 2010:1598–1614

Galioto TR (1985) The influence of elevation on the humic–fulvic acid ratio in soils of the Santa Catalina Mountains, Pima County, Arizona. M.S. thesis, University of Arizona, Tucson

Gavin DG (2001) Estimation of inbuilt age in radiocarbon ages of soil charcoal for fire history studies. Radiocarbon 43:27–44

Gessler PE, Moore ID, McKenzie NJ, Ryan PJ (1995) Soil-landscape modelling and spatial prediction of soil attributes. Int J Geogr Inf Syst 9:421–432

Golchin A, Oades JM, Skjemstad JO, Clarke P (1994) Study of free and occluded particulate organic matter in soils by solid-state ^{13}C CP/MAS NMR spectroscopy and scanning electron microscopy. Aust J Soil Res 32:285–309

Gonzalez-Perez JA, Gonzalez-Vila FJ, Almendros G, Knicker H (2004) The effect of fire on soil organic matter- a review. Environ Int 30:855–870. doi:10.1016/j.envint.2004.02.003

Hancock GR, Murphy D, Evans KG (2010) Hillslope and catchment scale soil organic carbon concentration: an assessment of the role of geomorphology and soil erosion in an undisturbed environment. Geoderma 155:36–45

Heckman K, Throckmorton H, Clingemsith C, Javier Gonzalez Vila F, Horwath WR, Knicker H, Rasmussen C (2014) Factors affecting the molecular structure and mean residence time of occluded organics in a lithosequence of soils under ponderosa pine. Soil Biol Biochem 77:1–11

Homann PS, Kapchinske JS, Boyce A (2007) Relations of mineral-soil C and N to climate and texture: regional differences within the conterminous USA. Biogeochemistry 85:303–316. doi:10.1007/s10533-007-9139-6

Hook P, Burke I (2000) Biogeochemistry in a shortgrass landscape: control by topography, soil texture, and microclimate. Ecology 81:2686–2703

Iniguez JM, Swetnam TW, Yool SR (2008) Topography affected landscape fire history patterns in southern Arizona, USA. For Ecol Manag 256:295–303

Iniguez JM, Swetnam TW, Baisan CH (2016) Fire history and moisture influences on historical forest age structure in the sky islands of southern Arizona, USA. J Biogeogr 43:85–95

Intergovernmental Panel on Climate Change (IPCC) (2013) The physical science basis. Contribution of Working group I to the fifth assessment report of the intergovernmental panel on climate change. Cambridge University Press, Cambridge, UK

Jobbágy EG, Jackson RB (2000) The vertical distribution of soil organic carbon and its relation to climate and vegetation. Ecol Appl 10:423–436

Kalbitz K, Schwesig D, Rethemeyer J, Matzner E (2005) Stabilization of dissolved organic matter by sorption to the mineral soil. Soil Biol Biochem 37:1319–1331

Kane ES, Valentine DW, Schuur EAG, Dutta K (2005) Soil carbon stabilization along climate and stand productivity gradients in black spruce forests of interior Alaska. Can J For Res 35:2118–2129

Lal R (2004) Carbon sequestration in dryland ecosystems. Environ Manag 33:528–544. doi:10.1007/s00267-003-9110-9

Landi A, Anderson DW, Mermut AR (2003) Organic carbon storage and stable isotope composition of soils along a grassland to forest environmental gradient in Saskatchewan. Can J Soil Sci 83:405–414

Lybrand RA, Rasmussen C (2014) Linking soil element-mass-transfer to microscale mineral weathering across a semiarid environmental gradient. Chem Geol 381:26–39

Lybrand RA, Rasmussen C (2015) Quantifying climate and landscape position controls on soil development in semi-arid ecosystems. Soil Sci Soc Am J 79:104–116

McClaran MP, Moore-Kucera J, Martens DA, van Haren J, Marsh SE (2008) Soil carbon and nitrogen in relation to shrub size and death in a semi-arid grassland. Geoderma 145:60–68

McFarlane KJ, Torn MS, Hanson PJ, Porras RC, Swanston CW, Callaham MA, Guilderson TP (2013) Comparison of soil organic matter dynamics at five temperate deciduous forests with physical fractionation and radiocarbon measurements. Biogeochemistry 112:457–476

Meier IC, Leuschner C (2010) Variation of soil and biomass carbon pools in beech forests across a precipitation gradient. Glob Chang Biol 16:1035–1045

Michalzik B, Tipping E, Mulder J, Gallardo Lancho JF, Matzner E, Bryant CL, Clarke N, Lofts S, Vicente Esteban MA (2003) Modelling the production and transport of dissolved organic carbon in forest soils. Biogeochemistry 66:241–264

Natelhoffer KJ, Fry B (1988) Controls on natural nitrogen-15 and carbon-13 abundances in forest soil organic matter. Soil Sci Soc Am J 52:1633–1640

Neff JC, Asner GP (2001) Dissolved organic carbon in terrestrial ecosystems: synthesis and a model. Ecosystems 4:29–48

Nicolau JM, Sole-Benet A, Puigdefabregas J, Gutierrez L (1996) Effects of soil and vegetation on runoff along a catena in semi-arid Spain. Geomorphology 14:297–309

North PF (1976) Towards an absolute measurement of soil structural stability using ultrasound. J Soil Sci 27:451–459

Pacala SW et al (2001) Consistent land- and atmosphere-based U.S. carbon sink estimates. Science 292:2316. doi:10.1126/science.1057320

Pelletier JD et al (2013) Coevolution of nonlinear trends in vegetation, soils, and topography with elevation and slope aspect: a case study in the sky islands of southern Arizona. J Geophys Res 118:741–758. doi:10.1002/jgrf.20046

Rasmussen C (2006) Distribution of soil organic and inorganic carbon pools by biome and soil taxa in Arizona. Soil Sci Soc Am J 70:256–265

Rasmussen C (2008) Mass balance of carbon cycling and mineral weathering across a semiarid environmental gradient. Geochim Cosmochim Acta 72:A778

Rasmussen C, White DA (2010) Vegetation effects on soil organic carbon quality in an arid hyperthermic ecosystem. Soil Sci 175:438–446

Rasmussen C, Torn MS, Southard RJ (2005) mineral assemblage and aggregates control carbon dynamics in a California conifer forest. Soil Sci Soc Am J 69:1711

Rasmussen C, Matsuyama N, Dahlgren RA, Southard RL, Brauer N (2007) Soil genesis and mineral transformation across an environmental gradient on andesitic lahar. Soil Sci Soc Am J 71:225

Rasmussen C, Dahlgren RA, Southard RJ (2010) Basalt weathering and pedogenesis across an environmental gradient in the southern Cascade Range, California, USA. Geoderma 154:473–485

Rawls WJ (1983) Estimating soil bulk density from particle size analysis and organic matter content. Soil Sci 135:123–125. doi:10.1097/00010694-198302000-00007

Rosenbloom NA, Harden JW, Neff JC, Schimel DS (2006) Geomorphic control of landscape carbon accumulation. J Geophys Res 111:G01004

Rumpel C, Kögel-Knabner I (2011) Deep soil organic matter—a key but poorly understood component of terrestrial C cycle. Plant Soil 338:143–158

Sanborn P, Geertsema M, Jull AJT, Hawkes B (2006) Soil and sedimentary charcoal evidence for Holocene forest fires in an inland temperate rainforest, east-central British Columbia, Canada. Holocene 16:415–427

Sanderman J, Amundson R (2008) A comparative study of dissolved organic carbon transport and stabilization in California forest and grassland soils. Biogeochemistry 92:41–59

Schiff SL, Aravena R, Trumbore SE, Dillon PJ (1990) Dissolved organic carbon cycling in forested watersheds: a carbon isotope approach. 26:2949–2957

Schimel D, Stillwell MA, Woodmansee RG (1985) Biogeochemistry of C, N, and P in a soil catena of the shortgrass steppe. Ecology 66:276–282

Schrumpf M, Kaiser K, Guggenberger G, Persson T, Kogel-Knaber I, Schulze E-D (2013) Storage and stability of organic carbon in soils as related to depth, occlusion within aggregates, and attachment to minerals. Biogeosciences 10:1675–1691

Seager R, Ting M, Held I, Kushnir Y, Lu J, Vecchi G, Huang H-P, Harnik N, Leetmaa A, Lau N-C, Li C, Velez J, Naik N (2007) Model projections of an imminent transition to a more arid climate in southwestern North America. Science 316:1181–1184

Sohi SP, Mahieu N, Arah JRM, Powlson DS, Madari B, Gaunt JL (2001) A procedure for isolating soil organic matter fractions suitable for modeling. Soil Sci Soc Am J 65:1121–1128

Soil Survey Staff (2010) Keys to soil taxonomy, 11th edn. U.S. Government Print Office, Washington, DC

Stephens SL, Finney MA, Shantz H (2004) Bulk density and fuel loads of ponderosa pine and white fir forest floors: impacts of leaf morphology. Northwest Sci 78:93–100

Swanston CW, Caldwell BA, Homann PS, Ganio L, Sollins P (2002) Carbon dynamics during a long-term incubation of separate and recombined density fractions from seven forest soils. Soil Biol Biochem 34:1121–1130

Swanston CW, Torn MS, Hanson PJ, Southon JR, Garten CT, Hanlon EM, Ganio L (2005) Initial characterization of processes of soil carbon stabilization using forest stand-level radiocarbon enrichment. Geoderma 128:52–62

Thornthwaite CW, Mather JR (1957) Instructions and tables for computing potential evapotranspiration and the water balance. Publ Climatol 10(3):185–311

Torn MS, Swanston CW, Castanha C, Trumbore SE (2009) Storage and turnover of organic matter in soil. In: Nicola Senesi, Baoshan Xing and PMH (eds) Biophys. Process. Involv. Nat. Nonliving Org. Matter Environ. Syst. John Wiley & Sons, Inc., pp 219–273

Torri D, Poesen J, Monaci F, Busoni E (1994) Rock fragment content and fine soil bulk density. Catena 23:65–71. doi:10.1016/0341-8162(94)90053-1

Trumbore SE, Davidson EA, Barbosa de Camargo P, Nepstad DC, Martinelli LA (1995) Belowground cycling of carbon in forests and pastures of Eastern Amazonia. Glob Bio 9:515–528

Trumbore SE, Chadwick OA, Amundson R (1996) Rapid exchange between soil carbon and atmospheric carbon dioxide driven by temperature change. Science 272(80):393–396

van Wagtendonk JW, Benedict JM, Sydoriak WM (1998) Dual bed characteristics of Sierra Nevada conifers. West J Appl For 13:73–84

Vogel JS (1987) C-14 background levels in an accelerator mass-spectrometry system. Radiocarbon 29:323–333

Von Lützow M, Kögel-Knabner I, Ludwig B, Matzner E, Flessa H, Ekscmitt K, Guggenberger G, Marschner B, Kalbitz K (2008) Stabilization mechanisms of organic matter in four temperate soils: development and application of a conceptual model. J Plant Nutr Soil Sci 171:111–124

Wagai R, Mayer LM, Kitayama K (2009) Nature of the "occluded" low-density fraction in soil organic matter studies: a critical review. Soil Sci Plant Nutr 55:13–25

Webster KL, Creed IF, Bourbonnière RA, Beall FD (2008) Controls on the heterogeneity of soil respiration in a tolerant hardwood forest. J Geophys Res 113:G03018

White DA, Welty-Bernard A, Rasmussen C, Schwartz E (2009) Vegetation controls on soil organic carbon dynamics in an arid, hyperthermic ecosystem. Geoderma 150:214–223

Whittaker R, Niering W (1965) Vegetation of the Santa Catalina Mountains, Arizona: a gradient analysis of the south slope. Ecology 46:429–452

Whittaker R, Niering W (1975) Vegetation of the Santa Catalina Mountains, Arizona. V. Biomass, production, and diversity along the elevation gradient. Ecology 56:771–790

Whittaker RH, Buol SW, Niering WA, Havens YH (1968) A soil and vegetation pattern in the Santa Catalina Mountains, Arizona. Soil Sci 105:440–450

Yoo K, Amundson R, Heimsath AM, Dietrich WE (2006) Spatial patterns of soil organic carbon on hillslopes: integrating geomorphic processes and the biological C cycle. Geoderma 130:47–65